Water Research 165 (2019) 115001

Contents lists available at ScienceDirect

Water Research

journal homepage: www.elsevier.com/locate/watres

Assessment of the chlorine demand and disinfection byproduct formation potential of surface waters via satellite remote sensing

Yiling Chen [a], William A. Arnold [a], Claire G. Griffin [b, 1], Leif G. Olmanson [c], Patrick L. Brezonik [a], Raymond M. Hozalski [a, *]

[a] Department of Civil, Environmental, and Geo- Engineering, University of Minnesota, 500 Pillsbury Drive SE, Minneapolis, MN, 55455-0116, United States
[b] Department of Ecology, Evolution, and Behavior, University of Minnesota, 1987 Upper Buford Circle, St. Paul, MN, 55108-6097, United States
[c] Department of Forest Resources, University of Minnesota, 1530 Cleveland Avenue North, St. Paul, MN, 55108-6112, United States

ARTICLE INFO

Article history:
Received 17 June 2019
Received in revised form
14 August 2019
Accepted 18 August 2019
Available online 21 August 2019

Keywords:
Colored dissolved organic matter
Disinfection byproducts
Chlorine demand
Satellite remote sensing
Surface water quality
Drinking water source

ABSTRACT

The ability of satellites to assess surface water quality indicators such as colored dissolved organic matter (CDOM) suggests that remote sensing could be a useful tool for evaluating water treatability metrics in considering potential drinking water supplies. To explore this possibility, 24 surface water samples were collected throughout Minnesota, USA with wide ranging values of CDOM (a_{440}; 0.41–27.9 m^{-1}), dissolved organic carbon (DOC; 5.5–47.6 mg/L) and specific ultraviolet absorbance at 254 nm ($SUVA_{254}$; 1.3–5.1 L/mg-M). Laboratory experiments were performed to quantify chlorine demand and the formation of two classes of halogenated disinfection byproducts (DBPs), trihalomethanes (THMs) and haloacetic acids (HAAs), using the uniform formation conditions (UFC) test. Chlorine demand and THM_{UFC} were linearly correlated with CDOM ($R^2 = 0.97$ and 0.91, respectively), indicating that CDOM is a useful predictor of these parameters. On the other hand, data comparing di- and tri-HAA_{UFC} with CDOM were better fit by a logarithmic relationship ($R^2 = 0.73$ and 0.87, respectively), while mono-HAA_{UFC} was linearly correlated with CDOM ($R^2 = 0.46$) but only for low-to moderately-colored waters ($a_{440} \leq 11\ m^{-1}$). The correlations relating chlorine demand and DBP_{UFC} values with CDOM were coupled with satellite CDOM assessments to estimate chlorine demand and DBP_{UFC} values for all surface waters larger than 0.05 km^2 in the state of Minnesota, USA. The resulting maps suggest that only 21.8% of Minnesota lakes would meet both the THM and HAA maximum contaminant levels, but only when pre-disinfection treatment removes 75% of DBP precursors. There are limitations to determining CDOM using satellites for high color surface waters ($a_{440} > 11\ m^{-1}$), however, leading to underpredicted values for CDOM, chlorine demand, and DBP_{UFC}. Overall, the results demonstrate the potential benefits of satellite remote sensing for assessing potential drinking water sources and water treatability metrics.

1. Introduction

Dissolved organic matter (DOM) originates primarily from two natural sources, production by aquatic organisms (autochthonous) and leaching of decaying terrestrial plant matter (allochthonous) (Thurman, 2012). DOM is also derived from anthropogenic sources such as wastewater effluent and agricultural and urban runoff. Colored dissolved organic matter (CDOM) is the portion of DOM that absorbs light at a specific wavelength, commonly 420 or 440 nm for freshwaters and 412 nm for marine waters (Brezonik et al., 2015). CDOM is primarily composed of humic and fulvic acids that contain abundant unsaturated carbon-carbon bonds, including aromatic moieties, which are known to absorb light in the ultraviolet (UV) and visible wavelength ranges (Del Castillo and Miller, 2008; Shank et al., 2005). CDOM is a major water quality driver because of its ability to mobilize metals (McKnight and Bencala, 1990) and hydrophobic chemicals, act as a photosensitizer for aquatic photochemistry (Gerecke et al., 2001), and control aquatic ecosystem processes (e.g., decrease light penetration) (Houser, 2006; Sommaruga, 2001; Thrane et al., 2014). Although not directly harmful to human health, DOM in source waters, including the CDOM fraction, can have negative effects on the cost

* Corresponding author.
E-mail address: hozalski@umn.edu (R.M. Hozalski).
[1] Current address: Department of Environmental Sciences, University of Virginia, Clark Hall, 291 McCormick Road, Charlottesville, VA, 22905, United States.

https://doi.org/10.1016/j.watres.2019.115001
0043-1354/

and effectiveness of water treatment operations and the finished water quality. It increases the consumption of water treatment chemicals such as coagulants (Sharp et al., 2006) and fouls membranes used for filtration (Zularisam et al., 2006). Furthermore, it reacts with chemical disinfectants such as free chlorine leading to the formation of potentially toxic disinfection byproducts (DBPs) (Beggs et al., 2009; Bellar et al., 1974; Eikebrokk et al., 2004; Herzsprung et al., 2012; Ledesma et al., 2012; Sedlak and von Gunten, 2011). Thus, CDOM plays a critical role in affecting both the chemistry of surface waters and their potential use as drinking water supplies.

The DOM content of surface waters is usually obtained by grab sampling and subsequent laboratory measurement of the dissolved organic carbon (DOC) concentration using a carbon analyzer or the UV/visible light absorbance using a spectrophotometer. Using such a sampling methodology to monitor DOM in large numbers of surface water bodies, on a regular (e.g., monthly) basis would be tedious and cost-prohibitive. Fortunately, investigations over the past 15 years have demonstrated the feasibility and practicality of using satellite remote sensing to measure CDOM in surface waters (Chen et al., 2017; Del Castillo and Miller, 2008; Fichot et al., 2015; Olmanson et al., 2016; Spyrakos et al., 2018; Xie et al., 2012; Zhu et al., 2014). By correlating measured CDOM to satellite reflectance, models can be developed for retrieving CDOM from publicly available satellite imagery. Such imagery, from satellite sensors such as the Landsat series, provide global coverage going back to 1972, potentially permitting researchers to quantify CDOM distributions and variability across long time periods and broad regional scales (Kutser, 2012). Moreover, CDOM typically is closely correlated with DOC in lakes and rivers (Griffin et al., 2018), and thus, the use of CDOM as a proxy of DOC for assessment of water treatability has important practical advantages over other water quality parameters because CDOM can be obtained via satellite remote sensing and is associated with humic substances that are known to have significant impacts on drinking water processes.

Given the importance of DOM in terms of water treatability, many researchers have developed empirical models that relate DOM content as DOC, UV absorbance at 254 nm (UV_{254}), or specific UV absorbance at 254 nm ($SUVA_{254}$) to various measures of water treatability, including chlorine demand (Abdullah et al., 2009; Yee et al., 2006), DBP formation (Amy et al., 1998; Chang et al., 1996; Rodriguez et al., 2000; Sohn et al., 2004; Watson et al., 1993), coagulant consumption (Van Leeuwen et al., 2005; Yang et al., 2010), and membrane fouling (Li and Chen, 2004; Liang et al., 2006). Such models are useful for process control because they permit important treatment concerns, such as water treatment chemical demand and DBP formation, to be predicted using parameters such as DOC and UV_{254} that can be measured in near-real time at a given location (Brinkman and Hozalski, 2011). We are unaware of any water treatability models that consider CDOM as a predictive variable. Developing models that consider CDOM as a variable instead of DOC or UV_{254} would enable the use of satellite remote sensing to assess potential water supplies and monitor the treatability of existing surface water supplies.

The objective of this study was to develop relationships between CDOM and two measures of water treatability, chlorine demand and DBP formation. A focus of this study was to compare trends for different classes of DBPs. Surface water samples were collected from 24 locations (in 20 lakes and 1 river) throughout Minnesota, and the formation of two regulated DBP classes (THMs and HAAs) upon chlorination was measured following the uniform formation conditions (UFC) test (Summers et al., 1996). The relationships between CDOM, DOC, UV–vis absorbance, and SUVA values for the water samples and their measured chlorine demand and DBP formation potentials (THMs, mono-, di- and tri-HAAs) were determined. The resulting models were coupled with Landsat-derived CDOM measurements to create statewide chlorine demand and DBP_{UFC} maps of Minnesota's lakes and rivers to demonstrate the possible use of satellite remote sensing for rapid large-scale assessments of water treatability.

2. Methods

2.1. Chemicals and reagents

A table of the chemicals used and their purities and suppliers is provided in the Supplementary Material (Table S1). All solutions were prepared using ultrapure water (18.2 MΩ-cm resistivity; Millipore).

2.2. Lake water sampling

Surface water samples were collected from 24 locations (20 lakes and 1 river; Lake Vermilion, Lake of the Woods, and Upper Red Lake were sampled twice in different locations) in four large ecoregions of Minnesota, USA – the Northern Lakes and Forests (NLF; 15 lakes), the North Central Hardwood Forests (NCHF; 4 lakes), the Northern Minnesota Wetlands (NMW; 4 lakes), and the Western Corn Belt Plains (WCBP; 1 lake) (Fig. S1). The adjacent NCHF and WCBP ecoregions were combined into a single category (NCHF + WCBP) because there was only one lake representing the WCBP and very little of its watershed is within the WCBP. The water samples were collected during the summer of 2016 and represent a subset of 412 samples collected from 299 locations (mostly lakes) across the Upper Midwest states of Minnesota, Wisconsin, and Michigan between 2014 and 2016 for analysis of CDOM and other water quality parameters (Griffin et al., 2018). The 24 water samples included in this investigation were selected to provide geographic diversity and a wide range of CDOM. Water samples typically were collected from a boat, canoe, or kayak at least 100 m from shore and within 1 m of the water surface by submerging acid-washed and triple-rinsed polycarbonate or high-density polyethylene (HDPE) containers to arm's length and then removing the cap. GPS coordinates of the sampling locations are provided in Table S2. Water samples for subsequent chlorine demand and DBP testing were filtered within a few hours of collection by pumping from the collection containers through 0.45 μm Geotech High Capacity capsule filters into clean containers. Aliquots of the filtered water for subsequent UV–visible light scans and DOC analysis were placed into separate pre-ashed 40 mL amber glass vials with the latter acidified to pH < 2 using 2 M HCl. All water samples were stored in the dark under refrigeration until further use. Chlorophyll-*a* was isolated from lake water samples by vacuum filtering onto 0.22 μm cellulose nitrate filters and stored frozen until analysis.

2.3. Chlorine demand and DBP formation testing

The chlorine demand of each water sample was determined by adding a stock solution of sodium hypochlorite (NaOCl) with 10% available chlorine at three different doses (Cl_2:DOC ratios of 1:1, 1.7:1 and 2:1) and measuring the residual concentration after incubating for 24 h at room temperature. The chlorine dose for subsequent UFC testing was selected to yield a free chlorine residual of 1.0 ± 0.4 mg Cl_2/L at the end of incubation. All glassware used in the chlorine demand and UFC experiments was cleaned by soaking in a concentrated hydrochloric acid bath (10%) for 24 h, rinsing with ultrapure water, and then baking at 550 °C for at least 6 h.

For UFC testing, triplicate aliquots of each water sample were

dosed with 2 mL/L borate buffer (1.0 M boric acid and 0.26 M sodium hydroxide, pH = 8.0) and adjusted to pH = 8.0 ± 0.2 using 1.0 M sulfuric acid or 1.0 M sodium hydroxide. After an incubation time of 24 h in the dark at 20 ± 1 °C, the chlorine residual was determined to ensure that it was within the required range. Samples outside the desired range were discarded and the test repeated with the chlorine dose adjusted as necessary. The chlorine residual was then quenched with Na_2SO_3 prior to extraction and analysis of DBPs.

2.4. Analytical methods

DOC was measured using a Shimadzu TOC L CSN analyzer after sparging the acidified samples with nitrogen gas. UV–Vis absorbance (A) scans from 200 to 800 nm were obtained using a Shimadzu 1601UV-PC dual beam spectrophotometer and 1 or 5 cm quartz cells. CDOM was calculated as the Napierian absorption coefficient at 440 nm (a_{440}) using the following equation:

$$a_{440}\left(m^{-1}\right) = 2.303 * A_{440}/l \quad (1)$$

where: A_{440} is the absorbance at 440 nm and l is the path length (m). Specific ultraviolet absorbance at 254 nm ($SUVA_{254}$) was calculated by normalizing the absorbance at 254 nm (UV_{254}) to the DOC concentration. Spectral slopes $S_{275-295}$ and $_{S350-400}$ were computed by fitting a linear regression to the natural logarithm of absorbance between the wavelength 275–295 and 350–400 nm, respectively. Chlorophyll a (chl a) was determined using a standard fluorometric method (Method 10200H) (Eaton et al., 2005). Total suspended solids (TSS) was obtained by filtering lake water through a pre-ashed 47 mm Whatman GF/F filter and normalizing the mass of dry residue by the volume of lake water filtered. Bromide concentration was determined via ion chromatography. Free chlorine was measured using the *N,N′*-diethyl-p-phenylenediamine (DPD) method and a Hach DR/890 portable colorimeter.

The concentrations of the THM_4 compounds (chloroform, TCM; bromodichloromethane, BDCM; dibromochloromethane, DBCM, and bromoform, TBM) and HAA_9 compounds (monochloroacetic acid, MCAA; dichloroacetic acid, DCAA; trichloroacetic acid, TCAA; monobromoacetic acid, MBAA; dibromoacetic acid, DBAA; tribromoacetic acid, TBAA; chlorodibromoacetic acid, CDBAA; bromochloroacetic acid, BCAA; and bromodichloroacetic acid, BDCAA) were determined using gas chromatography-microelectron capture detection (GC-μECD) according to modified USEPA Methods 551.1 and 552.3, respectively. Method details are provided in the SI. Specific chlorine demand and specific THM and HAA formation potentials (Specific THM_{UFC} and HAA_{UFC}) were calculated by normalizing chlorine demand, $THM_{UFC,}$ or HAA_{UFC} to the DOC concentration.

2.5. Data analysis and mapping

CDOM maps of Minnesota were created using an empirical model developed from Landsat 8 OLI Surface Reflectance (SR) Level-2 products from the Earth Resources Observation and Science (EROS) Center. The model was derived by step-wise regression to relate CDOM (a_{440}) data from 194 *in situ* measurements with corresponding spectral-radiometric data from four paths of clear Landsat 8 imagery from 2015 to 2016. The two-variable model used two band ratios: OLI3/OLI4 (green/red) and OLI4/OLI5 (red/near infrared):

$$\ln a_{440} = -5.478*(OLI3/OLI4) - 0.633*(OLI4/OLI5) + 8.135 \quad (2)$$

and had an R^2 of 0.77 and root-mean square error (RMSE) of 0.624 m^{-1}. This model was applied to 2016 clear Landsat 8 imagery with a few 2017 images to fill in areas not available in the 2016 imagery due to cloud cover. These areas were in western Minnesota and included portions of the Lake of the Woods and the Red Lakes, which are among Minnesota's largest lakes. Image processing was conducted using ERDAS Imagine software. Maps produced from multiple Landsat images were mosaicked to create the final state-wide CDOM map for Minnesota. The resulting pixel level CDOM maps together with experimentally obtained correlations (either Pearson for linear or LINEST for non-linear using Microsoft Excel) between chlorine demand and a_{440}, THM_{UFC} and a_{440}, and HAA_{UFC} and a_{440} were used to create state-wide maps for chlorine demand, THM_{UFC}, and HAA_{UFC}.

3. Results

3.1. Characteristics of lake waters

The water quality parameter values for the 24 water samples are summarized in Table S2. Observed ranges for key parameters are: CDOM (a_{440}): 0.41–27.9 m^{-1}, DOC: 5.5–47.6 mg/L, UV_{254}: 8.7–200 m^{-1}, $SUVA_{254}$: 1.3–5.1 L/mg-m, chlorophyll a: 1.1–14.4 μg/L, TSS: 0.7–13.9 mg/L, and pH: 7.1–8.8. Bromide concentrations were generally less than the limit of detection (0.01 mg/L) except for five samples with values ranging from 0.04 to 0.07 mg/L.

Relationships among the measured DOM parameters (a_{440}, DOC, UV_{254} and $SUVA_{254}$) are shown in Fig. 1. DOC and UV_{254} correlated linearly with a_{440} across the entire data range ($R^2 = 0.93$ and 0.98, respectively). The slopes and R^2 values for the Pearson correlations were similar when excluding three sampling sites with very high a_{440} values (South Sturgeon Lake, Lake Vermilion (Pike Bay)), and Upper Red Lake #2; data not shown). For $SUVA_{254}$, the greatest correlation coefficient values were obtained for linear regressions with log a_{440} ($R^2 = 0.88$) and log DOC ($R^2 = 0.78$). a_{440} did not correlate with other water quality indicators ($R^2 < 0.18$, and $p > 0.05$) including pH, TSS, chlorophyll a, and bromide (Table S2). Spectral slopes were computed from plots of the natural logarithm of absorbance vs. wavelength over the range 250–450 nm for each water sample (Fig. S2). Spectral slopes ($S_{275-295}$) among the water samples ranged from 0.013 to 0.028 nm^{-1}, but samples with visible color (i.e., $a_{440} > 3\ m^{-1}$) had a narrow range of $S_{275-295}$, 0.013–0.018 nm-1 $S_{350-400}$ also showed small variation ranging from 0.015 to 0.020 nm^{-1}, except for Mille Lacs Lake (low a_{440}) which had a $S_{350-400}$ of 0.009 nm^{-1}. The results indicated that the optical properties of a_{440} from moderate to high a_{440} waters are consistent across a large geographic range.

3.2. Chlorine demand

Chlorine demand values (mean ± standard deviation) for the 24 samples (Table S3) ranged from 3.68 ± 0.10 to 72.0 ± 0.17 mg Cl_2/L, with a mean of 14.9 mg Cl_2/L and a median of 8.58 mg Cl_2/L. In addition, the specific chlorine demand ranged from 0.56 ± 0.01 to 1.70 ± 0.01 mg Cl_2/mg C, and the mean and median specific chlorine demand were 0.97 and 0.85 mg Cl_2/mg C, respectively.

Chlorine demand exhibited a strong linear correlation with a_{440} ($R^2 = 0.97$; slope = 2.18 m-mg Cl_2/L), DOC ($R^2 = 0.98$; slope = 1.75 mg Cl_2/mg C), and UV_{254} ($R^2 = 0.99$; slope = 0.35 m-mg Cl_2/L) (Fig. 2), indicating that all three parameters are useful predictors of chlorine demand for the lakes. The slopes and R^2 values remained similar when the three lakes with very high a_{440} values were excluded from the regressions (data not shown). In addition, the organic carbon normalized specific chlorine demand correlated linearly with $SUVA_{254}$ ($R^2 = 0.84$; slope = 0.28 m-mg Cl_2/L).

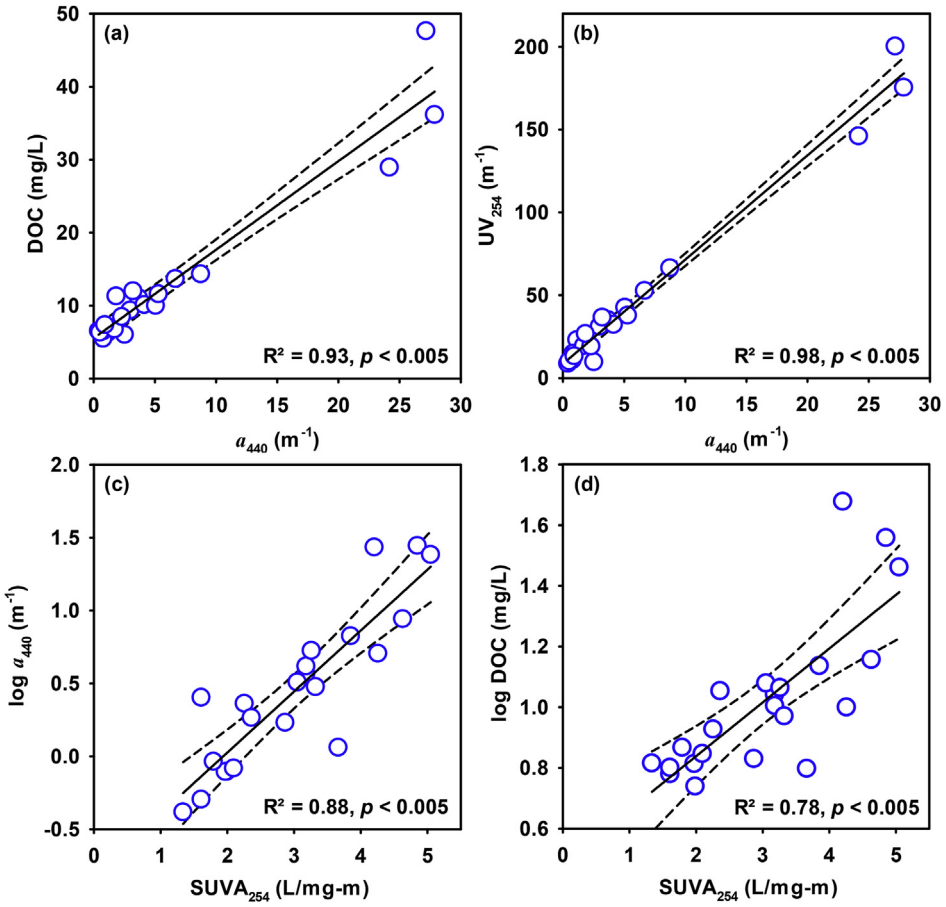

Fig. 1. Correlations among measured DOM parameters for selected Minnesota surface water samples (Table S1). The equations for the regressions shown are:
(a) DOC (mg/L) = 1.21 (±0.07) · a_{440} (m^{-1}) + 5.54 (±0.76);
(b) UV$_{254}$ (m^{-1}) = 6.30 (±0.20) · a_{440} (m^{-1}) + 8.57 (±2.03);
(c) log a_{440} (m^{-1}) = 0.42 (±0.05) · SUVA$_{254}$ (L/mg-m) − 0.81 (±0.16);
(d) log DOC (mg/L) = 0.18 (±0.03) · SUVA$_{254}$ (L/mg-m) + 0.49 (±0.10).
* Dashed lines represent 95% confidence intervals about the solid regression lines.

3.3. DBP formation

A wide range of DBP$_{UFC}$ values was found for the 24 waters (Table S3). South Sturgeon Lake, Lake Vermilion (Pike Bay), and Lake of the Woods (Muskeg Bay), which had the highest DOC levels, generated the maximum values for both THM$_{UFC}$ and HAA$_{UFC}$. The only THMs observed as chlorination products were TCM and BDCM (Fig. S3a). Although a few lakes contained bromide at concentrations exceeding the LOD, TCM was the dominant THM species formed in all samples, with mass concentration corresponding to >80% of the total THMs. The observed THM$_{UFC}$ values ranged from 104 ± 16.9 to 2019 ± 3.73 μg/L, and the mean THM$_{UFC}$ (421 μg/L) was much greater than the median THM$_{UFC}$ (264 μg/L). In contrast, specific THM$_{UFC}$ values ranged from 15.9 ± 0.95 to 55.9 ± 0.10 μg/mg C with comparable mean and median values (29.8 and 27.5 μg/mg C, respectively).

Five HAA species (MCAA, MBAA, DCAA, TCAA, BDCAA) were detected after chlorine dosing (Fig. S3b). In general, the total HAA$_{UFC}$ values were comparable to the total THM$_{UFC}$ values (Table S3). Although South Sturgeon Lake had the maximum HAA$_{UFC}$ (1366 ± 103 μg/L), Lake of the Woods (Fourmile Bay) had the highest specific HAA$_{UFC}$ (76.0 ± 2.19 μg/mg C). The lowest HAA$_{UFC}$ (47.0 ± 19.4 μg/L) and specific HAA$_{UFC}$ (7.22 ± 2.98 μg/mg C) were obtained for Island Lake. The mean HAA$_{UFC}$ was 469 μg/L, which is greater than the median value (363 μg/L), while the average specific HAA$_{UFC}$ (35.1 μg/mg C) was similar to the median value (32.0 μg/mg C). Distributions of HAAs were sorted into mono-, di- and tri-HAA species (Table S4) because each group apparently is formed from distinct precursors and chemical pathways (Chellam and Krasner, 2001). Consistent with many previous studies (Andrews et al., 2005; Krasner et al., 2006; Nuckols et al., 2001), the dominant HAA species were DCAA and TCAA, accounting for 74.6 ± 11.1% of the HAA$_5$ pool by mass, followed by MCAA. MBAA and BDCAA were detected but never exceeded 1% of the total HAA$_5$ pool (data not shown).

3.4. Correlations between DBP formation and CDOM

THM$_{UFC}$ exhibited a strong linear correlation with a_{440} ($R^2 = 0.91$; slope = 52.5 m-μg/L; Fig. 3a), indicating that CDOM (a_{440}) is a useful predictor of THM yields. Considering only the 21 waters with a_{440} below 9 m^{-1}, the R^2 decreased slightly ($R^2 = 0.84$), but the slope increased to 62.5 m-μg/L.

Regression analyses on the formation potentials of tri-, di- and mono-HAAs (Fig. 3b–d) in relation to a_{440} showed different trends than the THM$_{UFC}$- a_{440} relationship. Tri-HAA$_{UFC}$ correlated linearly with a_{440} ($R^2 = 0.87$) for low-to moderately-colored waters ($a_{440} \leq 11$ m^{-1}), but logarithmically when the entire data set was considered. The relationship between di-HAA$_{UFC}$ and a_{440} was similar, but with a lower slope in the low-to moderately-colored

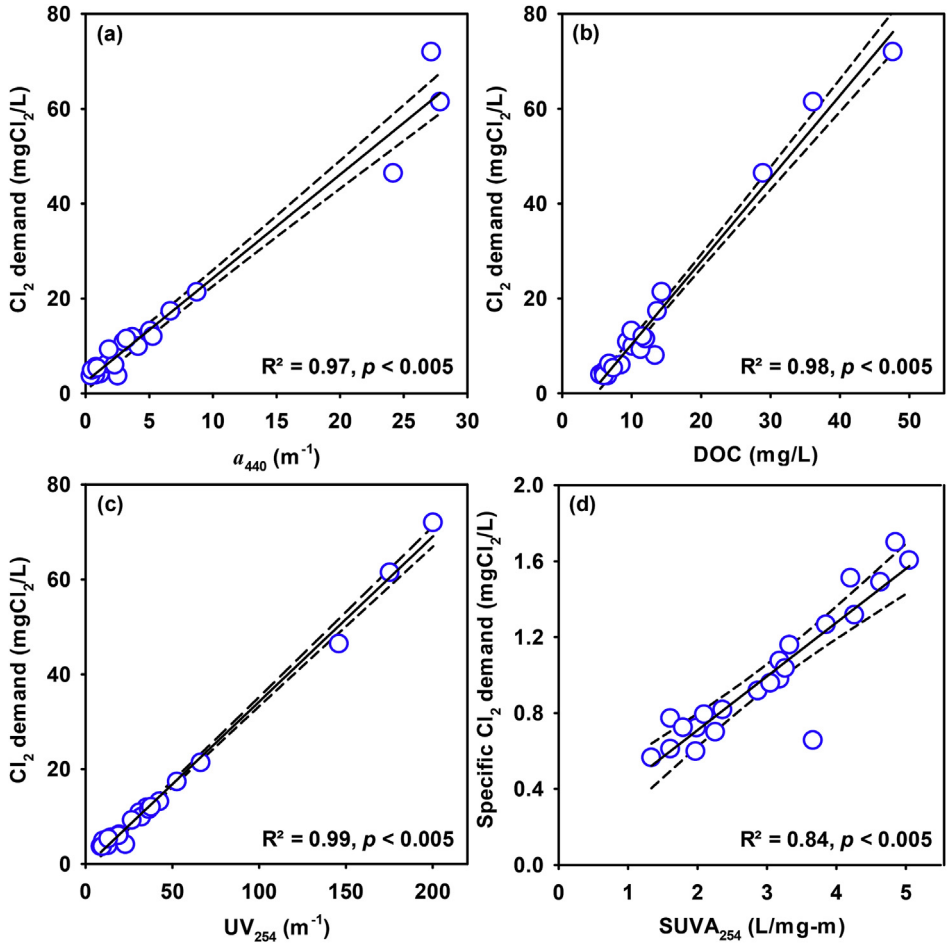

Fig. 2. Correlations of chlorine demand with CDOM (a_{440}), DOC, and UV_{254} (panels a–c) and specific chlorine demand with $SUVA_{254}$ (panel d). The regression equations are:
(a) Cl_2 demand ($mgCl_2$/L) = 2.18 (±0.09) · a_{440} (m^{-1}) + 2.47 (±0.90);
(b) Cl_2 demand ($mgCl_2$/L) = 1.75 (±0.06) · DOC (mg/L) - 7.17 (±0.92);
(c) Cl_2 demand ($mgCl_2$/L) = 0.35 (±0.01) · UV_{254} (m^{-1}) - 0.55 (±0.44);
(d) specific Cl_2 demand ($mgCl_2$/mgC) = 0.28 (±0.03) · $SUVA_{254}$ (L/mg-m) + 0.14 (±0.09).
* Dashed lines represent 95% confidence intervals about the solid regression lines.

lake waters ($R^2 = 0.73$; slope = 25.7 m-μg/L). Mono-HAA_{UFC}, on the other hand, exhibited a relatively weak correlation with a_{440}, with a linear correlation only observed for low-to moderately-colored waters ($R^2 = 0.46$; slope = 16.7 m-μg/L). Overall, these results agree with previous reports (Bond et al., 2009; Bull et al., 2006; Chang et al., 2006; Dickenson et al., 2008; Hua and Reckhow, 2007; Kanokkantapong et al., 2006; Kraus et al., 2010; Liang and Singer, 2003) that suggest the three classes of HAA species are formed from different precursors (see below).

3.5. Correlations between DBP formation and DOC or UV absorbance

DOC and UV_{254} have been widely used as surrogate parameters to predict DBP formation (Chowdhury et al., 2009; Sadiq and Rodriguez, 2004). Given the linear relationships between UV_{254} and a_{440} and between DOC and a_{440} (Fig. 1), it is not surprising that the strength of correlations between THM_{UFC}, di- and tri-HAA_{UFC} and DOC (Fig. S4) or UV_{254} (Fig. S5) were similar to those for a_{440}. THM_{UFC} exhibited a relatively strong linear relationship with DOC ($R^2 = 0.84$; slope = 40.3 μg/mgC) and UV_{254} ($R^2 = 0.91$; slope = 8.21 m-μg/L). Di- and tri-HAA_{UFC} relationships with DOC and UV_{254}, however, were best fit by logarithmic relationships ($R^2 = 0.87$ and 0.73, respectively, for DOC and $R^2 = 0.91$ and 0.82, respectively, for UV_{254}). When considering only the low-to moderately-colored lake waters, di- and tri-HAA_{UFC} increased linearly with increasing DOC ($R^2 = 0.67$ and 0.66, respectively) and UV_{254} ($R^2 = 0.90$ and 0.83, respectively). These results support the conclusion from previous studies that UV_{254} serves as a slightly better predictor of DBP formation than DOC concentration (Edzwald et al., 1985; Najm et al., 1994).

Mono-HAA_{UFC} correlated poorly with DOC and UV_{254} when all data were considered, but a stronger correlation was found for low-to moderately-colored waters ($R^2 = 0.69$, slope = 15.8 μg/mg C for DOC, Fig. S4d; $R^2 = 0.58$, slope = 2.73 m-μg/L, Fig. S5d for UV_{254}).

3.6. Correlations between specific DBP formation and SUVA

SUVA is often used as a proxy for the hydrophobicity, molecular weight (MW) and aromaticity of DOM (Dickenson et al., 2008; Hua and Reckhow, 2007; Singer et al., 2002). DOC-normalized or specific THM_{UFC} and tri-HAA_{UFC} exhibited relatively strong linear correlations with SUVA ($R^2 = 0.67$ and 0.65, respectively; slope = 7.57 and 8.17 m-μg/L, respectively; Fig. S6) suggesting that these DBPs are formed from UV absorbing organic matter (i.e., humic substances). Conversely, relatively weak correlations were observed

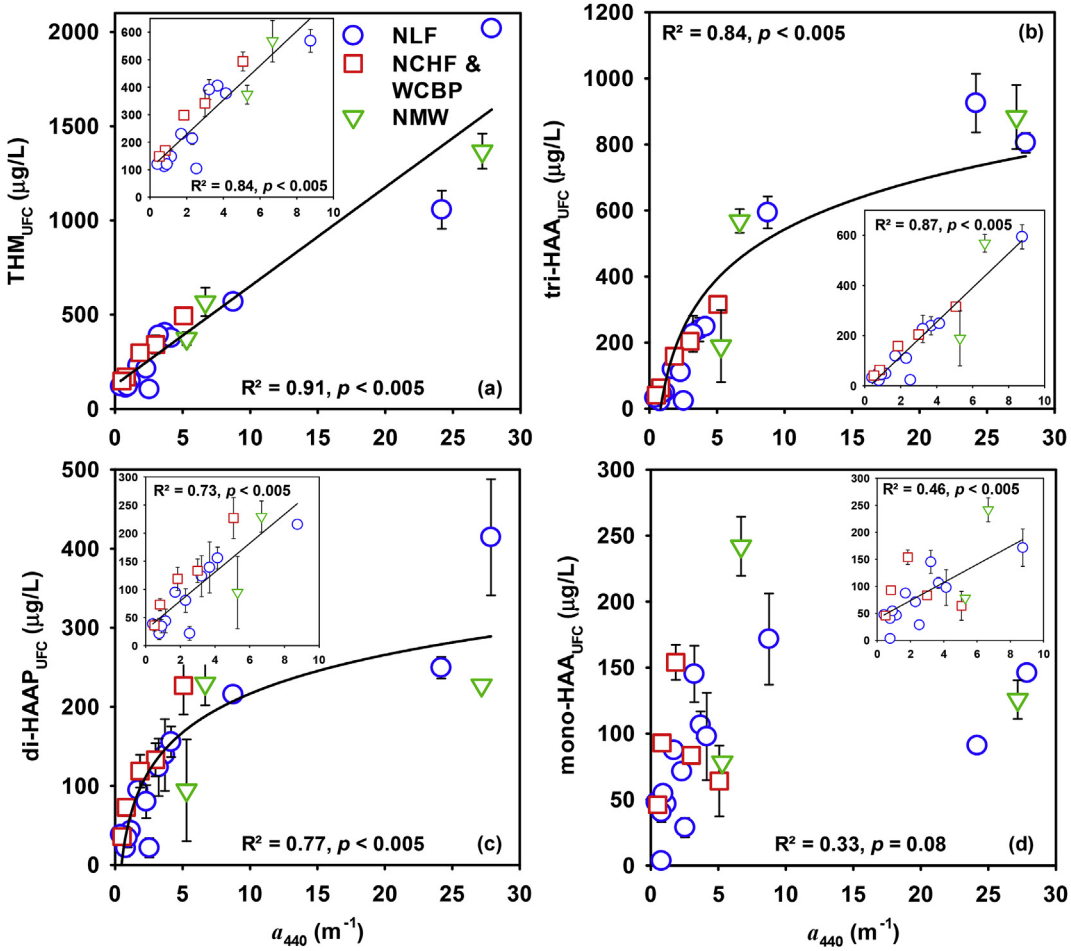

Fig. 3. Correlations of THM_{UFC}, tri-HAA_{UFC}, di-HAA_{UFC}, and mono-HAA_{UFC} with CDOM (a_{440}). The equations for the regressions are:
(a) THM_{UFC} (µg/L) = 52.5 (±3.67) · a_{440} (m^{-1}) + 127 (±37.9); THM_{UFC} (µg/L) for low a_{440} = 62.5 (±6.59) · a_{440} (m^{-1}) + 104 (±23.8);
(b) tri-HAA_{UFC} (µg/L) = 217 (±21.0) · ln a_{440} (m^{-1}) + 43.4 (±33.4); tri-HAA_{UFC} (µg/L) for low a_{440} = 68.3 (±6.34) · a_{440} (m^{-1}) − 19.0 (±22.9);
(c) di-HAA_{UFC} (µg/L) = 70.7 (±8.64) · ln a_{440} (m^{-1}) + 53.8 (±13.8); di-HAA_{UFC} (µg/L) for low a_{440} = 25.7 (±3.76) · a_{440} (m^{-1}) + 28.2 (±13.6);
(d) mono-HAA_{UFC} (µg/L) for low a_{440} = 16.7 (±4.41) · a_{440} (m^{-1}) + 40.3 (±15.9).

between SUVA and specific mono- and di-HAA_{UFC}. In addition, when lakes with SUVA exceeding 3 L/mg-m were considered, the mono-HAA yields started to decrease with increasing SUVA (Fig. S6d). These results imply that low UV absorbing organic matter (i.e., non-humic substances) contributed substantially to formation of mono- and di-HAA species.

3.7. Chlorine demand and DBP_{UFC} mapping

Using a_{440} data from satellite imagery and the correlations between chlorine demand and a_{440} (Fig. 2), THM_{UFC} and a_{440} (Fig. 3) and HAA_{UFC} and a_{440} (Fig. S7), state-wide maps for chlorine demand and DBP formation potentials were produced. The map for THM_{UFC} (Fig. 4) shows relatively high levels of THM_{UFC} (>400 µg/L) in lakes of northeastern Minnesota, especially within the NLF ecoregion. This result is not surprising as most Minnesota lakes with $a_{440} > 3\ m^{-1}$ are located in the NLF ecoregion. Lower THM_{UFC} values are predicted for the NCHF, NMW and WCBP ecoregions, and most lakes in these three ecoregions are relatively low in color. Consistent with the THM_{UFC} results, NLF lakes generally have higher levels of HAA_{UFC} (>480 µg/L) (Fig. S8) and chlorine demand (>5 $mgCl_2$/L) (Fig. S9). The distribution of DBP_{UFC} levels in the four ecoregions clearly reflected their current distributions of forested, urban and agricultural land uses. For example, the NLF ecoregion is extensively forested, with large areas of wetlands and open water. Undeveloped land covers 89% of the NLF ecoregion. In contrast, almost half of the NCHF ecoregion is cultivated, with forests and wetlands only making up 35% of land cover (Brezonik et al., 2019). The WCBP ecoregion is dominated by agricultural use (83% of land cover) but also contains some open grassland (Brezonik et al., 2019).

Comparisons of values of CDOM, chlorine demand, THM_{UFC}, and HAA_{UFC} estimated from satellite imagery versus experimentally measured values are shown in Fig. 5. The estimated values represent an average of the grid cell containing the physical sampling location and the neighboring cells. For lakes with CDOM values less than 10 m^{-1}, the plotted values for all parameters lie close to the 1:1 line (Fig. 5a), indicating that satellite remote sensing is capable of accurate assessing CDOM and CDOM-associated parameters such as THM_{UFC} in low to moderately-colored waters. The agreement was poor, however, for two lakes with very high CDOM levels ($a_{440} > 20\ m^{-1}$) (i.e., South Sturgeon Lake and Lake Vermilion (Pike Bay)), as the estimated CDOM, chlorine demand and DBP_{UFC} values were substantially less than the corresponding experimentally-measured values (Fig. 5a–d). In addition, negative HAA_{UFC} values were obtained for six low CDOM ($a_{440} < 2.5\ m^{-1}$) sampling sites (Fig. 5d). The latter results suggest that estimation of HAA_{UFC} using satellite remote sensing can be problematic for waters with very low color.

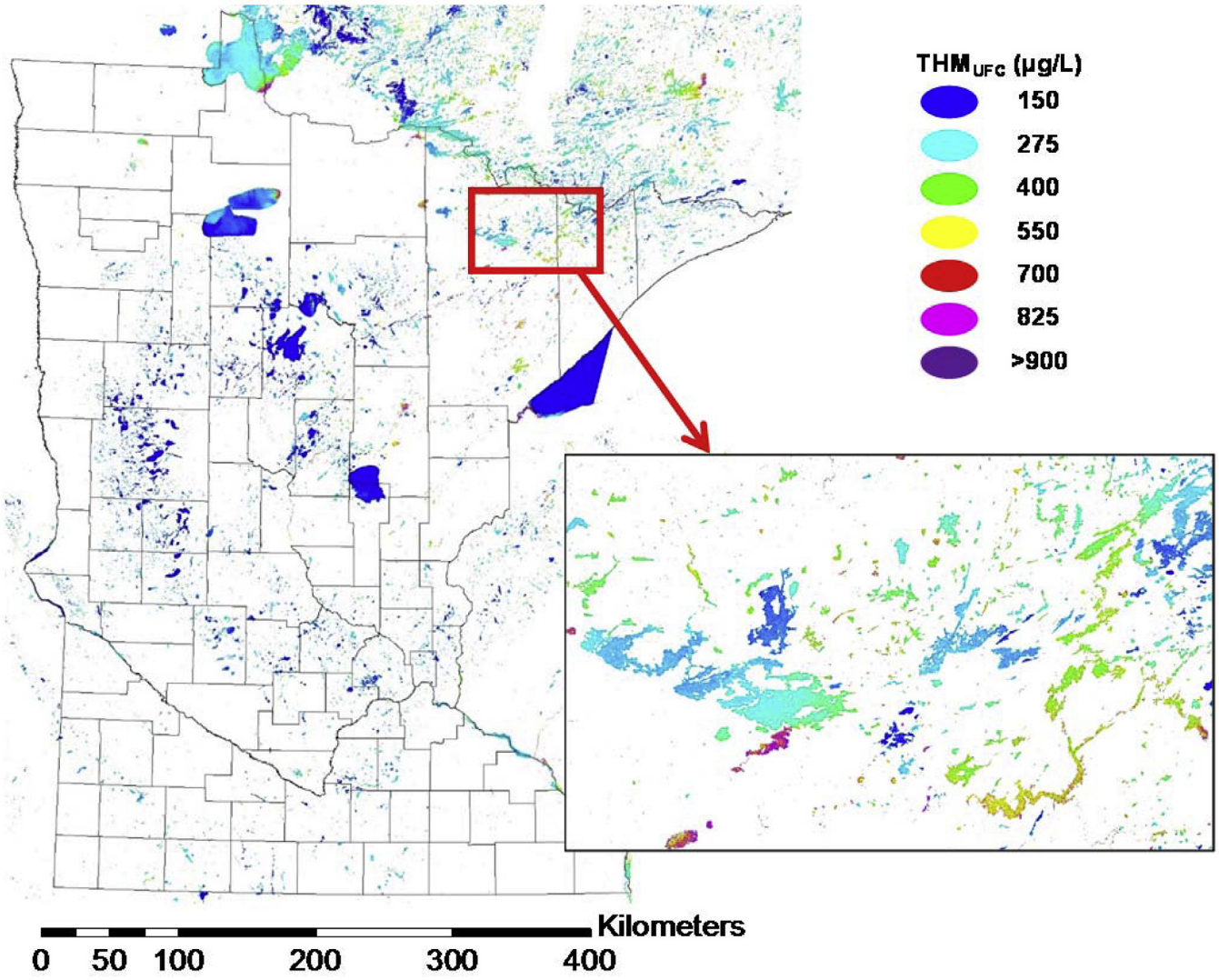

Fig. 4. Distribution of estimated lake THM_{UFC} concentrations in Minnesota lakes based on 2016 and 2017 Landsat 8 images. A zoom in of the Ely area in northeast Minnesota is shown in the inset figure.

Based on the USEPA Stage 1 Disinfectants and Disinfection Byproducts Rule, maximum contaminant levels for THM_4 and HAA_5 are 80 µg/L and 60 µg/L, respectively. As our DBP_{UFC} values are for raw lake water, lake-averaged CDOM values from the statewide CDOM mapping were used to estimate the percentage of lakes that would violate either or both abovementioned MCLs by assuming three potential levels of DBP precursor removal (25% (poor removal), 50% (conventional treatment), and 75% (enhanced coagulation); Fig. 6 and Table S7). Consequently, THM_4 concentrations in raw waters would be limited to 107, 160, and 320 µg/L, respectively; while for HAA_5 the limits would be 80, 120, and 240 µg/L, respectively. None of Minnesota's lakes ($n = 11{,}690$) would be expected to meet the THM_4 MCL assuming 25% precursor removal, but 62.4% of Minnesota lakes would meet the MCL assuming 75% precursor removal. The percentage of Minnesota lakes that would be expected to meet the HAA_5 MCL assuming 25% precursor removal was only 11.3% but increased to 21.8% for 75% removal. Finally, the percentage of Minnesota lakes that would be expected to meet both DBP MCLs was only 21.8% for 75% precursor removal. It is important to note, however, that this estimation considered only the number of lakes and not lake area or volume. Referring to the maps showing the distribution of DBP_{UFC} levels (Fig. 4 and Fig. S9), most lakes in some regions of Minnesota, such as the northeast, are not likely to be useful as drinking water sources because of their high color and potential to form high levels of DBPs even when reasonable precursor removals are assumed.

4. Discussion

4.1. CDOM as a predictor of chlorine demand DBP formation

Historically, predictive models for DBP formation include parameters such as DOC, UV_{254}, and $SUVA_{254}$, which are commonly used surrogates for DOM quantity and composition (Chowdhury et al., 2009; Sadiq and Rodriguez, 2004). Other parameters include pH, water temperature, chlorine dose, and reaction time. Most modeling efforts have focused on THM formation with considerably less work on HAA formation (Chowdhury et al., 2009; Sadiq and Rodriguez, 2004). For example (Singer and Chang, 1989), developed linear relationships between THM formation and UV_{254}. Other researchers have developed multivariate models to relate DBP concentrations to a combination of DOC and other variables

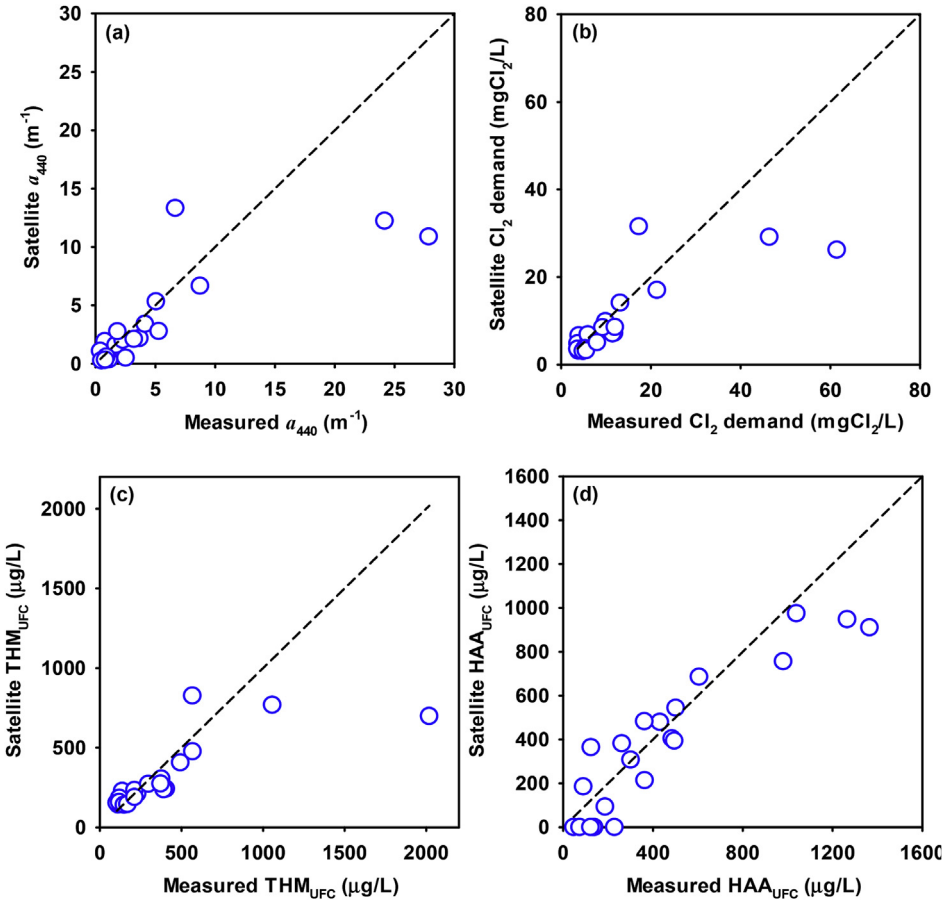

Fig. 5. Comparison of estimated (satellite) and measured values of (a) a_{440}, (b) chlorine demand; (c) THM formation potential (THM_{UFC}); and (d) HAA formation potential (HAA_{UFC}). The dashed line is a 1:1 line. The results for the Mississippi River and Upper Red #2 (at the mouth of the Tamarac River) were excluded from the plots because the riverine flows create highly dynamic conditions not suitable for comparisons with relatively infrequent satellite imagery. Negative HAA_{UFC} values were set to 0.

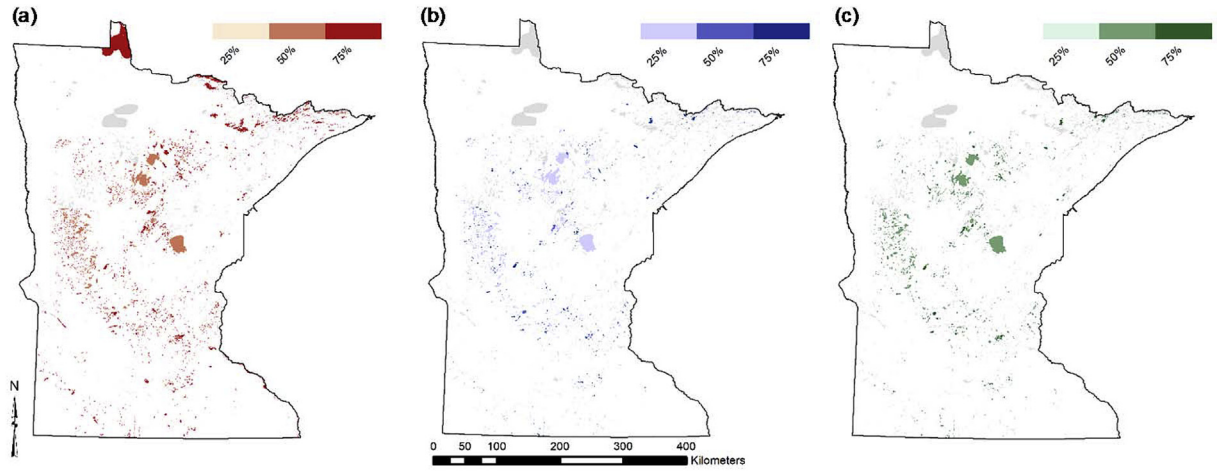

Fig. 6. Distribution of Minnesota lakes expected to meet the (a) THM_4 MCL; (b) HAA_5 MCL; (c) THM_4 and HAA_5 MCL at three potential levels of DBP precursor removal (25%, 50%, and 75%). The grey color shows the rest of lakes that violate either or both MCLs. Calculations were made based on the average of 2015 and 2016 Landsat derived a_{440} measurements, and the developed models correlating a_{440} and DBP formation potentials (THM_{UFC} and HAA_{UFC}).

including water temperature, bromide level, chlorine dose, and contact time (Amy et al., 1987; Sérodes et al., 2003). Such empirical models often have limited applicability given the narrow range of water qualities used for model development. DOC is a broad indicator of the concentration of DOM whereas UV_{254} represents specific structural characteristics and functional groups (Croue et al., 2000; Edzwald et al., 1985). $SUVA_{254}$ provides a relative proxy for the aromaticity of DOM, and as a result, its feasibility at predicting DBP formation highly depends on the relative importance of aromatic DOM in reacting with chlorine to form DBPs.

Unfortunately, neither DOC nor UV_{254} can be obtained directly from satellite observations. Although UV_{254} is an optical property that provides a sensitive measure of DOM content, UV irradiation is so strongly absorbed by the Earth's atmosphere that very little is reflected back to orbiting satellites.

CDOM (a_{440}), in contrast, is readily obtained from satellite observations because light in the visible and longer wavelength ranges is not as strongly absorbed by the atmosphere yet is sufficiently absorbed by CDOM to result in predictable shifts in the reflectance spectra. CDOM in the limnology literature refers to the color or light absorptivity of dissolved substances in water, which has implications for growth of phytoplankton and submerged vegetation (Gallegos, 2001; Geider, 1987), lake trophic status (Brezonik et al., 2005), and biogeochemical cycling of elements (Zepp et al., 2007). As such, CDOM is an important variable affecting lake and river ecology. The color of drinking water is important as an aesthetic parameter with a color maximum of 15 mg Pt/L (as measured by the cobalt-platinum method) in the USA (EPA, 2018) and generally correlates with light absorptivity.

We are unaware, however, of any reports in the literature regarding models for predicting DBP formation that use CDOM (a_{440}) as a proxy. The results of this study demonstrated strong correlations between a_{440} and THM_{UFC}, di-HAA_{UFC} and tri-HAA_{UFC}; indicating that CDOM can serve as a predictor of DBP formation. This has important implications for the use of satellite remote sensing to assess the suitability and treatability of surface waters as potential drinking water sources.

Unfortunately, mono-HAA_{UFC} did not correlate strongly with a_{440}, indicating that a_{440} alone may not be adequate for predicting mono-HAA formation in source waters. Total HAA_5, however, is reasonably well predicted using a_{440} ($R^2 = 0.85$; Fig. S7a) because mono-HAA_{UFC} accounted for less than 26% of the total HAA_5 pool. Thus, using this correlation between a_{440} and HAA_5 for HAA_{UFC} mapping is possible. Despite the issues with mono-HAA, CDOM is a reasonably good predictor of the formation of regulated DBPs upon chlorination.

4.2. DBP formation and correlations with UV_{254} and DOC

Reported values for THM_{UFC} and HAA_{UFC} typically range from 3 to 388 μg/L, but values as high as 1300 μg/L have been observed in a few cases (White et al., 2003; Zeng and Arnold, 2013). Additionally, values for THM and HAA formation potentials (THM_{FP} and HAA_{FP}) ranging from 20 to 450 μg/L have been reported (Bougeard et al., 2010; Gang et al., 2002; Hua and Reckhow, 2007; Lee et al., 2007; Summers et al., 1996; Zhao et al., 2016). DBP_{FP} is expected to be greater than DBP_{UFC} due to the higher chlorine doses and longer contact times in the formation potential test. Reported chlorine demand values also exhibit a wide range (2.0–108 mg Cl_2/L) (Gang et al., 2002; Zeng and Arnold, 2013; Zhao et al., 2016). The chlorine demand and DBP_{UFC} values determined in the present study fall into the above reported ranges, with the exception of a few waters containing DOC concentrations that were much greater than surface waters routinely used as drinking water supplies, including South Sturgeon Lake, Lake Vermilion (Pike Bay) and Lake of the Woods (Muskeg Bay). When the results were normalized to DOC to obtain specific chlorine demand and specific DBP_{UFC}, values from the present study (specific chlorine demand: 0.56 ± 0.01 to 1.70 ± 0.01 mg Cl_2/mg C, specific THM_{UFC}: 15.9 ± 0.95 to 55.9 ± 0.10 μg/mg C, specific HAA_{UFC}: 7.22 ± 2.98 to 76.0 ± 2.19 μg/mg C) were comparable with previously published values (specific chlorine demand: 0.5–1.8 mg Cl_2/mg C, specific DBP_{UFC}: 2.5–106 μg/mg C).

Previously reported correlations of chlorine demand and DBP formation potential with DOC, UV_{254}, and $SUVA_{254}$ were summarized (Table S6) to allow comparison with our findings. The slope of chlorine demand versus DOC in the present study (1.75 ± 0.06 mg Cl_2/mg C) was greater than previously published values (0.56–1.05 mg Cl_2/mg C) (Gang et al., 2002; Zeng and Arnold, 2013). The slope of the THM_{UFC} versus DOC plot in the present study (52.5 ± 3.67 μg/mg C) was also somewhat greater than values reported for raw waters (30–36 μg/mg C) (Gang et al., 2002; Summers et al., 1996), but much greater than that for treated (coagulation/filtration/ozone/GAC) waters (0.038 μg/mg C) (Bougeard et al., 2010). The slope of HAA_{UFC} versus UV_{254} observed in the present study was similar to previously reported values. The slope of HAA_{UFC} versus DOC in the present study, however, was greater than previously reported values, which is likely due to the different DBP precursors present in the tested waters. Thus, it appears that organic matter in the lakes of this study was often more reactive with free chlorine than those in previous investigations. Nevertheless, other differences in experimental conditions, such as chlorine contact time, pH, or water temperature, also could have played a role in the observed differences in specific chlorine demand and specific DBP_{UFC}.

4.3. Factors affecting DBP formation

Previous research has suggested that the hydrophobic or aromatic fractions of DOM are primarily responsible for the formation of THMs and HAAs (Bond et al., 2012; Kitis et al., 2002; Pan and Zhang, 2013; Zhai and Zhang, 2011). For example, humic substances (i.e., fulvic and humic acids), generally representing the major fraction of DOM in surface waters, are the main THM and HAA precursors (Leenheer and Croué, 2003; Reckhow and Singer, 1985). Specifically, 1,3-dihydroxybenzene structures, as phenolic aromatic moieties, preferentially generate THMs (Rook, 1977). Phenolic groups also are important TCAA precursors (Bond et al., 2009; Dickenson et al., 2008). Earlier research on chlorination of DOM fractions isolated from whole water samples indicated that DCAA precursors are more hydrophilic and lower in MW than TCAA precursors (Hua and Reckhow, 2007; Kanokkantapong et al., 2006; Liang and Singer, 2003), and aliphatic β-dicarbonyl moieties are key precursors in DCAA formation (Bond et al., 2009; Bull et al., 2006; Chang et al., 2006; Dickenson et al., 2008). Likewise, SUVA was an effective predictor for specific THMs and tri-HAA_{UFC} in our study suggesting that aromatic structures, such as phenolic groups, are the primary precursor of THMs and tri-HAAs (Singer et al., 2002). The weaker relationship observed between SUVA and specific di-HAA_{UFC} indicated that the di-HAA precursors are less aromatic, and aliphatic carbon may play a more important role in their formation than in that of tri-HAAs. SUVA was shown to be a poor indicator of mono-HAA formation, suggesting that non-humic substances are important precursors of mono-HAAs. Our findings lend further support to the finding that the mono-, di-, and tri-HAAs have different precursors and formation mechanisms upon chlorination.

Besides the nature and concentrations of DOM, the underlying causes of differences in speciation of DBPs in different waters could also include bromide ion concentration, chlorine dose and chlorination conditions (e.g., pH, contact time) (Panyapinyopol et al., 2005; Symons et al., 1996; Xie et al., 2006; Zhao et al., 2006). Bromide concentrations above 0.1 mg/L trigger concern about brominated DBP formation (Zhang et al., 2011) due to the formation of HOBr and its ability to react with DBP precursors. In our study, bromide was < LOD in most lakes, with a maximum of 0.066 mg/L in Lake Vermilion (Pike Bay), effectively limiting the generation of brominated DBPs. In addition, previous publications have shown that pH affects HAA and THM formation in opposite ways; THM formation increases with increasing pH, but HAA formation decreases with increasing pH (Singer et al., 1995).

4.4. Implications for use of satellite remote sensing for assessment of water treatability

The generally strong correlations between CDOM and chlorine demand or DBP_{UFC} suggests that satellite remote sensing is a useful technology for assessing the treatability of low-to moderately-colored surface waters with regard to chlorine demand and DBP formation. Furthermore, it might be possible to elucidate long-term trends in surface water treatability measures impacted by CDOM, such as chlorine demand, using historical Landsat imagery. Satellite remote sensing could also prove valuable in assessing other water treatability metrics, such as coagulant demand and membrane fouling, if the metrics are strongly linked to CDOM levels.

DBP_{UFC} values for two highly colored waters computed from satellite assessed CDOM values, however, were severely underestimated. High CDOM ($a_{440} > 11\ m^{-1}$) results in strong light absorption with very little reflected light reaching the satellite sensors. The resulting weak signal leads to substantial errors in predicted CDOM. To date, most investigations on satellite remote sensing have focused on CDOM levels up to $10\ m^{-1}$ (Kutser et al., 2005a, 2005b). Olmanson et al. (2016), however, reported models that considered lakes with high CDOM levels (a_{440} up to $18\ m^{-1}$). The models showed an increase in uncertainty at higher a_{440}, which is consistent with our results. In addition, other factors such as interference from suspended solids could also affect satellite CDOM values. Hence, our approach for assessing DBP_{UFC} from satellite imagery should be used with caution for high CDOM and optically complex waters.

The chlorine demand and DBP formation experiments in this study were performed on raw lake water samples and the maps created reflect these raw water values. Certainly, the characteristics of organic matter and specific precursors present in the raw waters in this study will differ from treated waters that have undergone organic matter removal via coagulation/flocculation. Coagulation processes can remove 50% or more of the DOC with even greater reductions in UV_{254}, suggesting that coagulation preferentially removes higher MW and more aromatic DOM (Chowdhury et al., 2009). Further, the removal of DOM increases the bromide to organic carbon ratio, which can shift the distribution of DBPs toward more brominated species (Chowdhury et al., 2009). Filtered, but untreated, surface waters were used in our UFC tests because models have been developed to relate CDOM to light reflectance values from lake surfaces obtained by satellites. Thus, maps showing predictions of Minnesota lakes likely to meet DBP MCLs were prepared assuming various levels of precursor removal (25%, 50%, and 75%) that could be obtained with conventional treatment or enhanced coagulation. The resulting state-wide assessments suggested that a very low percentage of Minnesota lakes, especially in the heavily forested NLF ecoregion, would meet both THM and HAA MCLs unless aggressive pre-disinfection treatment was done to remove at least 75% of DBP precursors.

Finally, another potential limitation of this work is that satellites are measuring near surface parameters while water utilities often withdraw water from greater depths, such as below the thermocline in stratified lakes. The effect of this discrepancy in where measurements are made in the water body and where the water is withdrawn on predictions of CDOM and CDOM-related parameters is uncertain, but believed to be relatively minor, compared to other water quality parameters that exhibit strong depth dependence such as chlorophyll *a*. Vertical profiles of CDOM in a few colored Minnesota lakes showed small to moderate changes with depth (Brezonik et al., 2019).

5. Conclusions

Twenty-four surface water samples were collected throughout Minnesota, USA with wide ranging values of CDOM (a_{440}; $0.41-27.9\ m^{-1}$), dissolved organic carbon (DOC; 5.5–47.6 mg/L) and specific ultraviolet absorbance at 254 nm ($SUVA_{254}$; 1.3–5.1 L/mg-M). Laboratory experiments were performed to quantify chlorine demand and the formation of two classes of halogenated disinfection byproducts (DBPs), trihalomethanes (THMs) and haloacetic acids (HAAs), using the uniform formation conditions (UFC) test. The correlations relating chlorine demand and DBP_{UFC} values with CDOM were coupled with satellite CDOM assessments to estimate chlorine demand, THM_{UFC}, and HAA_{UFC} values for all surface waters larger than $0.05\ km^2$ in the state of Minnesota, USA. The main conclusions from this work are as follows:

- Chlorine demand and THM_{UFC} correlated linearly with CDOM (a_{440}) and di- and tri-HAA_{UFC} correlated logarithmically with CDOM when all sampled waters were considered. For low-to moderately-colored waters ($a_{440} \leq 11\ m^{-1}$), a linear relationship provided a good fit ($R^2 \geq 0.73$) for all of these cases and a moderate fit ($R^2 = 0.46$) for mono-HAA_{UFC} versus CDOM. Thus, CDOM (a_{440}) appears to be an effective predictor of chlorine demand, THM_{UFC}, and HAA_{UFC}.
- CDOM (a_{440}), chlorine demand, THM_{UFC}, and HAA_{UFC} did not correlate with conventional water quality indicators including TSS and chlorophyll *a*.
- For highly colored surface waters ($a_{440} > 11\ m^{-1}$), CDOM and DBP_{UFC} values were substantially underestimated from the satellite data due to various factors, including strong absorption of incident light resulting in a weak signal received by the satellite sensors.
- Overall, the results demonstrate that satellite remote sensing could be a useful tool for assessing water treatability metrics like chlorine demand and DBP formation, especially for low-to moderately-colored lakes.

Declaration of competing interest

The authors declare that they have no known competing financial interests or personal relationships that could have appeared to influence the work reported in this paper.

Acknowledgments

The authors gratefully acknowledge funding from the State of Minnesota's Environment and Natural Resources Trust Fund (ENRTF) and National Science Foundation (CBET-1510332). The authors thank Noah Germolus for assistance with bromide concentration measurements.

Appendix A. Supplementary data

Supplementary data to this article can be found online at https://doi.org/10.1016/j.watres.2019.115001.

References

Abdullah, M.P., Yee, L.F., Ata, S., Abdullah, A., Ishak, B., Abidin, K.N.Z., 2009. The study of interrelationship between raw water quality parameters, chlorine demand and the formation of disinfection by-products. Phys. Chem. Earth 34, 806–811. https://doi.org/10.1016/j.pce.2009.06.014.

Amy, G.L., Chadik, P.A., Chowdhury, Z.K., 1987. Developing models for predicting trihalomethane formation potential and kinetics. Journal-American Water Work. Assoc. 79, 89–97.

Amy, G.L., Siddiqui, M., Ozekin, K., Zhu, H.W.H.W., Wang, C., 1998. Empirical Based Models for Predicting Chlorination and Ozonation Byproducts: Haloacetic Acids, Chloral Hydrate, and Bromate. Report CX 819579. U.S. Environmental Protection Agency, Cincinnati, Ohio.

Andrews, R.C., Alam, Z., Hofmann, R., Lachuta, L., Cantwell, R., Andrews, S., Moffet, E., Gagnon, G.A., Rand, J., Chauret, C., 2005. Impact of Chlorine Dioxide

on Transmission, Treatment, and Distribution System Performance. American Water Works Association.
Beggs, K.M.H., Summers, R.S., McKnight, D.M., 2009. Characterizing chlorine oxidation of dissolved organic matter and disinfection by-product formation with fluorescence spectroscopy and parallel factor analysis. J. Geophys. Res. Biogeosciences 114.
Bellar, T.A., Lichtenberg, J.J., Kroner, R.C., 1974. The occurrence of organohalides in chlorinated drinking waters. Journal-American Water Work. Assoc. 66, 703–706.
Bond, T., Goslan, E.H., Parsons, S.A., Jefferson, B., 2012. A critical review of trihalomethane and haloacetic acid formation from natural organic matter surrogates. Environ. Technol. Rev. 1, 93–113. https://doi.org/10.1080/09593330.2012.705895.
Bond, T., Henriet, O., Goslan, E.H., Parsons, S.A., Jefferson, B., 2009. Disinfection byproduct formation and fractionation behavior of natural organic matter surrogates. Environ. Sci. Technol. 43, 5982–5989.
Bougeard, C.M.M., Goslan, E.H., Jefferson, B., Parsons, S.A., 2010. Comparison of the disinfection by-product formation potential of treated waters exposed to chlorine and monochloramine. Water Res. 44, 729–740.
Brezonik, P., Menken, K.D., Bauer, M., 2005. Landsat-based remote sensing of lake water quality characteristics, including chlorophyll and colored dissolved organic matter (CDOM). Lake Reservoir Manag. 21, 373–382. https://doi.org/10.1080/07438140509354442.
Brezonik, P.L., Bouchard, R.W., Finlay, J.C., Griffin, C.G., Olmanson, L.G., Anderson, J.P., Arnold, W.A., Hozalski, R., 2019. Color, chlorophyll a, and suspended solids effects on Secchi depth in lakes: implications for trophic state assessment. Ecol. Appl. 29, e01871. https://doi.org/10.1002/eap.1871.
Brezonik, P.L., Olmanson, L.G., Finlay, J.C., Bauer, M.E., 2015. Factors affecting the measurement of CDOM by remote sensing of optically complex inland waters. Remote Sens. Environ. 157, 199–215. https://doi.org/10.1016/j.rse.2014.04.033.
Brinkman, B.M., Hozalski, R.M., 2011. Temporal variation of NOM and its effects on membrane treatment. Journal-American Water Work. Assoc. 103, 98–106.
Bull, R., Reckhow, D., Rotello, V., Bull, O.M., Kim, J., 2006. Use of Toxicological and Chemical Models to Prioritize DBP Research, Water Intelligence Online. https://doi.org/10.1016/j.jns.2013.07.1872.
Chang, E.E., Chao, S., Chiang, P., Lee, J., 1996. Effects of chlorination on THMs formation in raw water. Toxicol. Environ. Chem. 56, 211–225.
Chang, E.E., Chiang, P.C., Chao, S.H., Lin, Y.L., 2006. Relationship between chlorine consumption and chlorination by-products formation for model compounds. Chemosphere 64, 1196–1203.
Chellam, S., Krasner, S.W., 2001. Disinfection byproduct relationships and speciation in chlorinated nanofiltered waters. Environ. Sci. Technol. 35, 3988–3999. https://doi.org/10.1021/es010775n.
Chen, J., Zhu, W.N., Tian, Y.Q., Yu, Q., 2017. Estimation of colored dissolved organic matter from Landsat-8 imagery for complex inland water: case study of Lake Huron. IEEE Trans. Geosci. Remote Sens. 55, 2201–2212. https://doi.org/10.1109/TGRS.2016.2638828.
Chowdhury, S., Champagne, P., McLellan, P.J., 2009. Models for predicting disinfection byproduct (DBP) formation in drinking waters: a chronological review. Sci. Total Environ. 407, 4189–4206. https://doi.org/10.1016/j.scitotenv.2009.04.006.
Croue, J.-P., Korshin, G.V., Benjamin, M.M., 2000. Characterization of Natural Organic Matter in Drinking Water. American Water Works Association.
Del Castillo, C.E., Miller, R.L., 2008. On the use of ocean color remote sensing to measure the transport of dissolved organic carbon by the Mississippi River Plume. Remote Sens. Environ. 112, 836–844. https://doi.org/10.1016/j.rse.2007.06.015.
Dickenson, E.R.V., Summers, R.S., Croué, J.P., Gallard, H., 2008. Haloacetic acid and trihalomethane formation from the chlorination and bromination of aliphatic β-Dicarbonyl acid model compounds. Environ. Sci. Technol. 42, 3226–3233. https://doi.org/10.1021/es0711866.
Eaton, A.D., Clesceri, L.S., Rice, E.W., Greenberg, A.E., Franson, M., 2005. APHA: Standard Methods for the Examination of Water and Wastewater. Centen. In: APHA, AWWA (Eds.). WEF, Washington, DC.
Edzwald, J.K., Becker, W.C., Wattier, K.L., 1985. Surrogate parameters for monitoring organic matter and THM precursors. Journal-American Water Work. Assoc. 77, 122–132.
Eikebrokk, B., Vogt, R.D., Liltved, H., 2004. NOM increase in Northern European source waters: discussion of possible causes and impacts on coagulation/contact filtration processes. Water Sci. Technol. Water Supply 4, 47–54.
EPA, 2018. 2018 2018 Drinking Water Standards and Advisory.
Fichot, C.G., Downing, B.D., Bergamaschi, B.A., Windham-Myers, L., Marvin-DiPasquale, M., Thompson, D.R., Gierach, M.M., 2015. High-resolution remote sensing of water quality in the San Francisco Bay–Delta estuary. Environ. Sci. Technol. 50, 573–583.
Gallegos, C.L., 2001. Calculating optical water quality targets to restore and protect submersed aquatic vegetation: overcoming problems in partitioning the diffuse attenuation coefficient for photosynthetically active radiation. Estuaries 24, 381–397.
Gang, D.D., Segar Jr., R.L., Clevenger, T.E., Banerji, S.K., 2002. Using chlorine demand to predict TTHM and HAA9 formation. Journal-American Water Work. Assoc. 94, 76–86.
Geider, R.J., 1987. Light and temperature dependence of the carbon to chlorophyll a ratio in microalgae and cyanobacteria: implications for physiology and growth of phytoplankton. New Phytol. 106, 1–34.
Gerecke, A.C., Canonica, S., Muller, S.R., Scharer, M., Schwarzenbach, R.P., 2001. Quantification of dissolved natural organic matter (DOM) mediated phototransformation of phenylurea herbicides in lakes. Environ. Sci. Technol. 35, 3915–3923. https://doi.org/10.1021/es010103x.
Griffin, C.G., Finlay, J.C., Brezonik, P.L., Olmanson, L., Hozalski, R.M., 2018. Limitations on using CDOM as a proxy for DOC in temperate lakes. Water Res. 144, 719–727. https://doi.org/10.1016/j.watres.2018.08.007.
Herzsprung, P., von Tümpling, W., Hertkorn, N., Harir, M., Büttner, O., Bravidor, J., Friese, K., Schmitt-Kopplin, P., 2012. Variations of DOM quality in inflows of a drinking water reservoir: linking of van Krevelen diagrams with EEMF spectra by rank correlation. Environ. Sci. Technol. 46, 5511–5518.
Houser, J.N., 2006. Water color affects the stratification, surface temperature, heat content, and mean epilimnetic irradiance of small lakes. Can. J. Fish. Aquat. Sci. 63, 2447–2455.
Hua, G., Reckhow, D.A., 2007. Characterization of disinfection byproduct precursors based on hydrophobicity and molecular size. Environ. Sci. Technol. 41, 3309–3315.
Kanokkantapong, V., Marhaba, T.F., Panyapinyophol, B., Pavasant, P., 2006. FTIR evaluation of functional groups involved in the formation of haloacetic acids during the chlorination of raw water. J. Hazard Mater. 136, 188–196.
Kitis, M., Karanfil, T., Wigton, A., Kilduff, J.E., 2002. Probing reactivity of dissolved organic matter for disinfection by-product formation using XAD-8 resin adsorption and ultrafiltration fractionation. Water Res. 36, 3834–3848.
Krasner, S.W., Weinberg, H.S., Richardson, S.D., Pastor, S.J., Chinn, R., Sclimenti, M.J., Onstad, G.D., Thruston, A.D., 2006. Occurrence of a new generation of disinfection byproducts. Environ. Sci. Technol. 40, 7175–7185.
Kraus, T.E.C., Anderson, C.A., Morgenstern, K., Downing, B.D., Pellerin, B.A., Bergamaschi, B.A., 2010. Determining sources of dissolved organic carbon and disinfection byproduct precursors to the McKenzie River, Oregon. J. Environ. Qual. 39, 2100–2112.
Kutser, T., 2012. The possibility of using the Landsat image archive for monitoring long time trends in coloured dissolved organic matter concentration in lake waters. Remote Sens. Environ. 123, 334–338.
Kutser, T., Pierson, D.C., Kallio, K.Y., Reinart, A., Sobek, S., 2005a. Mapping lake CDOM by satellite remote sensing. Remote Sens. Environ. 94, 535–540. https://doi.org/10.1016/j.rse.2004.11.009.
Kutser, T., Pierson, D.C., Tranvik, L., Reinart, A., Sobek, S., Kallio, K., 2005b. Using satellite remote sensing to estimate the colored dissolved organic matter absorption coefficient in lakes. Ecosystems 8, 709–720. https://doi.org/10.1007/s10021-003-0148-6.
Ledesma, J.L.J., Köhler, S.J., Futter, M.N., 2012. Long-term dynamics of dissolved organic carbon: implications for drinking water supply. Sci. Total Environ. 432, 1–11. https://doi.org/10.1016/j.scitotenv.2012.05.071.
Lee, W., Westerhoff, P., Croué, J.-P., 2007. Dissolved organic nitrogen as a precursor for chloroform, dichloroacetonitrile, N-nitrosodimethylamine, and trichloronitromethane. Environ. Sci. Technol. 41, 5485–5490.
Leenheer, J.A., Croué, J.-P., 2003. Characterizing aquatic dissolved organic matter. Environ. Sci. Technol. 37 (1), 19A–26A. https://doi.org/10.1021/es032333c.
Li, C.-W., Chen, Y.-S., 2004. Fouling of UF membrane by humic substance: effects of molecular weight and powder-activated carbon (PAC) pre-treatment. Desalination 170, 59–67.
Liang, L., Singer, P.C., 2003. Factors influencing the formation and relative distribution of haloacetic acids and trihalomethanes in drinking water. Environ. Sci. Technol. 37, 2920–2928.
Liang, S., Song, L., Tao, G., Kekre, K.A., Seah, H., 2006. A modeling study of fouling development in membrane bioreactors for wastewater treatment. Water Environ. Res. 78, 857–864.
McKnight, D.M., Bencala, K.E., 1990. The chemistry of iron, aluminum, and dissolved organic material in three acidic, metal-enriched, mountain streams, as controlled by watershed and in-stream processes. Water Resour. Res. 26, 3087–3100.
Najm, I.N., Patania, N.L., Jacangelo, J.G., Krasner, S.W., 1994. Evaluating surrogates for disinfection by-products. J. Am. Water Work. Assoc. 86, 98–106.
Nuckols, J., Rossman, L.A., Singer, P.C., 2001. Development of Exposure Assessment Methods for THM and HAA in Water Distribution Systems. American Water Works Association.
Olmanson, L.G., Brezonik, P.L., Finlay, J.C., Bauer, M.E., 2016. Comparison of Landsat 8 and Landsat 7 for regional measurements of CDOM and water clarity in lakes. Remote Sens. Environ. 185, 119–128. https://doi.org/10.1016/j.rse.2016.01.007.
Pan, Y., Zhang, X., 2013. Four groups of new aromatic halogenated disinfection byproducts: effect of bromide concentration on their formation and speciation in chlorinated drinking water. Environ. Sci. Technol. 47, 1265–1273.
Panyapinyopol, B., Marhaba, T.F., Kanokkantapong, V., Pavasant, P., 2005. Characterization of precursors to trihalomethanes formation in Bangkok source water. J. Hazard Mater. 120, 229–236.
Reckhow, D.A., Singer, P.C., 1985. Mechanisms of organic halide formation during fulvic acid chlorination and implications with respect to preozonation. Water Chlorination Chem. Environ. Impact Heal. Eff. 5, 1229–1257.
Rodriguez, M.J., Sérodes, J., Morin, M., 2000. Estimation of water utility compliance with trihalomethane regulations using a modelling approach. J. Water Supply Res. Technol. 49, 57–73.
Rook, J.J., 1977. Chlorination reactions of fulvic acids in natural waters. Environ. Sci. Technol. 11, 478–482.
Sadiq, R., Rodriguez, M.J., 2004. Disinfection by-products (DBPs) in drinking water and predictive models for their occurrence: a review. Sci. Total Environ. 321,

21–46.
Sedlak, D.L., von Gunten, U., 2011. The chlorine dilemma. Science 331 (80), 42–43.
Sérodes, J.-B., Rodriguez, M.J., Li, H., Bouchard, C., 2003. Occurrence of THMs and HAAs in experimental chlorinated waters of the Quebec City area (Canada). Chemosphere 51, 253–263.
Shank, G.C., Zepp, R.G., Whitehead, R.F., Moran, M.A., 2005. Variations in the spectral properties of freshwater and estuarine CDOM caused by partitioning onto river and estuarine sediments. Estuar. Coast Shelf Sci. 65, 289–301.
Sharp, E.L., Parsons, S.A., Jefferson, B., 2006. Seasonal variations in natural organic matter and its impact on coagulation in water treatment. Sci. Total Environ. 363, 183–194.
Singer, P.C., Chang, S.D., 1989. Correlations between trihalomethanes and total organic halides formed during water treatment. Journal-American Water Work. Assoc. 81, 61–65.
Singer, P.C., Obolensky, A., Greiner, A., 1995. DBPs in chlorinated North Carolina drinking waters. J. Am. Water Work. Assoc. 87, 83–92.
Singer, P.C., Weinberg, H.S., Brophy, K., 2002. Relative Dominance of Haloacetic Acids and Trihalomethanes in Treated Drinking Water. American Water Works Association.
Sohn, J., Amy, G., Cho, J., Lee, Y., Yoon, Y., 2004. Disinfectant decay and disinfection by-products formation model development: chlorination and ozonation by-products. Water Res. 38, 2461–2478.
Sommaruga, R., 2001. The role of solar UV radiation in the ecology of alpine lakes. J. Photochem. Photobiol. B Biol. 62, 35–42.
Spyrakos, E., O'Donnell, R., Hunter, P.D., Miller, C., Scott, M., Simis, S.G.H., Neil, C., Barbosa, C.C.F., Binding, C.E., Bradt, S., 2018. Optical types of inland and coastal waters. Limnol. Oceanogr. 63, 846–870.
Summers, R.S., Hooper, S.M., Shukairy, H.M., Solarik, G., Owen, D., 1996. Assessing DBP yield: uniform formation conditions. Journal-American Water Work. Assoc. 88, 80–93.
Symons, J.M., Krasner, S.W., Sclimenti, M.J., Simms, L.A., Sorensen Jr., H.W., Spietel Jr., G.E., Diehl, A.C., 1996. Influence of bromide ion on trihalomethane and haloacetic acid formation. Disinfect. by-products water Treat. Chem. their Form. Control 91–130.
Thrane, J.-E., Hessen, D.O., Andersen, T., 2014. The absorption of light in lakes: negative impact of dissolved organic carbon on primary productivity. Ecosystems 17, 1040–1052.
Thurman, E.M., 2012. Organic Geochemistry of Natural Waters. Springer Science & Business Media.
Van Leeuwen, J., Daly, R., Holmes, M., 2005. Modeling the treatment of drinking water to maximize dissolved organic matter removal and minimize disinfection by-product formation. Desalination 176, 81–89.
Watson, M., American Water Works Association, Water Industry Technical Action Fund (U.S.), 1993. Mathematical Modeling of the Formation of THMs and HAAs in Chlorinated Natural Waters, Final Report. Water Industry Technical Action Fund. American Water Works Association.
White, D.M., Garland, D.S., Narr, J., Woolard, C.R., 2003. Natural organic matter and DBP formation potential in Alaskan water supplies. Water Res. 37, 939–947.
Xie, H., Aubry, C., Bélanger, S., Song, G., 2012. The dynamics of absorption coefficients of CDOM and particles in the St. Lawrence estuarine system: biogeochemical and physical implications. Mar. Chem. 128, 44–56.
Xie, S., Wen, D., Shi, D., Tang, X., 2006. Reduction of precursors of chlorination by-products in drinking water using fluidized-bed biofilm reactor at low temperature. Biomed. Environ. Sci. 19, 360.
Yang, Z., Gao, B., Yue, Q., 2010. Coagulation performance and residual aluminum speciation of Al2 (SO4) 3 and polyaluminum chloride (PAC) in Yellow River water treatment. Chem. Eng. J. 165, 122–132.
Yee, L.F., Abdullah, M.P., Ata, S., Ishak, B., 2006. Dissolved organic matter and its impact on the chlorine demand of treated water. Malaysian J. Anal. Sci. 10, 243–250.
Zeng, T., Arnold, W.A., 2013. Clustering chlorine reactivity of haloacetic acid precursors in inland lakes. Environ. Sci. Technol. 48, 139–148.
Zepp, R.G., Erickson Iii, D.J., Paul, N.D., Sulzberger, B., 2007. Interactive effects of solar UV radiation and climate change on biogeochemical cycling. Photochem. Photobiol. Sci. 6, 286–300.
Zhai, H., Zhang, X., 2011. Formation and decomposition of new and unknown polar brominated disinfection byproducts during chlorination. Environ. Sci. Technol. 45, 2194–2201.
Zhang, J., Yu, J., An, W., Liu, J., Wang, Y., Chen, Y., Tai, J., Yang, M., 2011. Characterization of disinfection byproduct formation potential in 13 source waters in China. J. Environ. Sci. 23, 183–188.
Zhao, Y., Yang, H. wei, Liu, S. ting, Tang, S., Wang, X. mao, Xie, Y.F., 2016. Effects of metal ions on disinfection byproduct formation during chlorination of natural organic matter and surrogates. Chemosphere 144, 1074–1082. https://doi.org/10.1016/j.chemosphere.2015.09.095.
Zhao, Z.-Y., Gu, J.-D., Fan, X.-J., Li, H.-B., 2006. Molecular size distribution of dissolved organic matter in water of the Pearl River and trihalomethane formation characteristics with chlorine and chlorine dioxide treatments. J. Hazard Mater. 134, 60–66.
Zhu, W., Yu, Q., Tian, Y.Q., Becker, B.L., Zheng, T., Carrick, H.J., 2014. An assessment of remote sensing algorithms for colored dissolved organic matter in complex freshwater environments. Remote Sens. Environ. 140, 766–778.
Zularisam, A.W., Ismail, A.F., Salim, R., 2006. Behaviours of natural organic matter in membrane filtration for surface water treatment—a review. Desalination 194, 211–231.